

Chapter

Electrochemical Behavior of Cellulose Nanofibrils Functionalized with Dicyanovinyl Groups

*Robson V. Pereira, Thais E. Gallina,
Marcelo A. Pereira-da-Silva, Kênia S. Freitas
and Aparecido J. de Menezes*

Abstract

Cellulose is considered one of the most important renewable sources of biopolymers on Earth. It has attracted widespread attention due to its physical–chemical characteristics, such as biocompatibility, low toxicity, biodegradability, low density, high strength, stability in organic solvents, in addition to having hydroxyl groups, which enable its chemical modification. In this study, cellulose nanofibrils (CNFs) were functionalized with dicyanovinyl groups through nucleophilic vinylic substitution (SNV) and used as electrocatalyst in electrochemical of carbon dioxide (CO₂) reduction. Results indicate that introducing dicyanovinyl groups into the structure of nanocellulose increases electrocatalytic activity as compared to that of pure nanocellulose, shifting the onset potential of the electrochemical CO₂ reduction reaction to more positive values as compared to those for the reaction with argon. The atomic force microscopy (AFM) images show no changes in the morphology of CNFs after chemical modification.

Keywords: cellulose nanofibrils, nucleophilic vinylic substitution, electrochemical CO₂ reduction

1. Introduction

The most abundant biopolymer on Earth, cellulose displays wide chemical variability due to the functionalization capability of its hydroxyl groups, via chemical and physical reactions. Moreover, cellulose exhibits diverse morphologies, found in the hierarchical constructions that constitute plants. Cellulose is mainly found in plant cell walls, but it can also be found in other living beings, such as bacteria, fungi, and even in some species of sea mammals [1, 2].

From the standpoint of chemical structure, this biopolymer belongs to the carbohydrate group, classified as a linear polysaccharide consisting of β-D-glycopyranose units joined by β-1,4 glycosidic bonds. As a result, cellulose exhibits a high molecular weight ranging from about 50,000 to 2.5 million g/mol, depending on its source [3]. The repetitive unit of cellulose, known as cellobiosis, is a cellulose dimer (**Figure 1**).

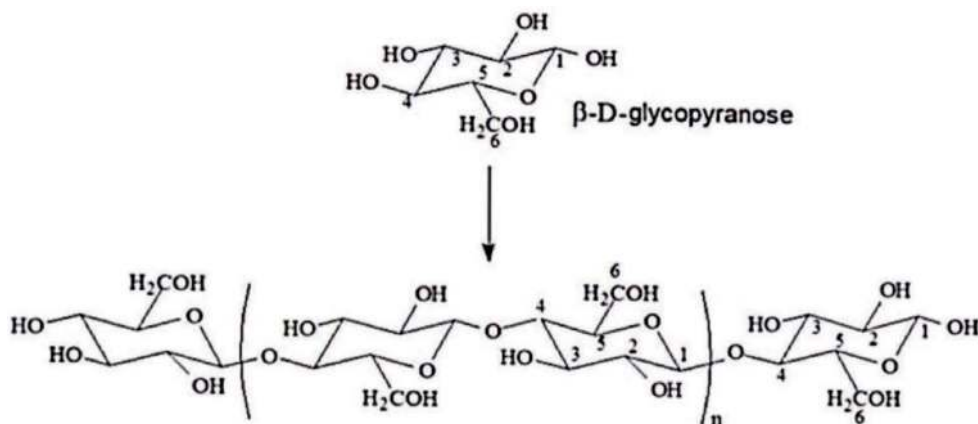


Figure 1.
Molecular structure of cellulose.

Each of these individual chains clusters into larger units, called fibrils or microfibrils, which in turn clump together and form cellulose fibers. This organization may present amorphous regions, in which fibers exhibit an undefined arrangement, or highly organized segments with fibers arranged parallel to each other. Notwithstanding other arrangements, crystalline and amorphous stretches constitute the most common fiber configurations in the polymeric structure of cellulose [1].

The degree of polymerization (DP) of this semi-crystalline biopolymer varies according to the raw material used to obtain it and the method used for its extraction. For instance, wood pulp has a DP between 10,000 and 15,000 glycosidic units, while values for cellulose of bacterial origin range from 2,000 to 6,000 [4].

At nanoscale, cellulose can be obtained by chemical or physical methods or both. Cellulose nanofibrils are usually obtained by physical methods, e.g., high shear rate mechanical treatment, whereas cellulose nanocrystals are usually obtained by chemical methods, e.g., acid hydrolysis. The difference between mechanically-produced nanocellulose and chemically-produced cellulose is that the former can reach a length of up to 2 μm , while the latter, in addition to being crystalline, exhibits a length of the order of 150 nm [5, 6].

Besides its physical-chemical properties, such as low cost, biodegradability, renewability, low toxicity, and stability in organic solvents, nanocellulose exhibits a high aspect ratio and a high specific surface area. These properties combined promote its use in nanocomposites [7–9], hydrogels and aerogels [10, 11], biomedical products [12, 13], pharmaceuticals [14], environmental applications [15], and electrochemistry. In the latter case, it is used mainly in sensors [16], transistors, and solar cells [17, 18].

The introduction of strong electron withdrawing groups such as malononitrile groups in dyes and polymers has been reported in the literature [19, 20], and the presence of these groups leads to Intramolecular Charge Transfer (ICT), increasing the electron density in dicyano groups.

Electrochemical CO_2 reduction is not only an effective way of lowering CO_2 concentrations in the atmosphere, but it is also advantageous. CO_2 can be effectively reduced to renewable fuels, such as ethanol, methane, and methanol, which can contribute to meeting today's growing demand for renewable energy sources [21, 22]. So, some studies on CO_2 reduction catalysis have used conducting polymers as polyethylenimine (PEI) [23], and polyaniline (Pan) [24] that causes an effect of reducing catalytic overpotential and increasing current density and efficiency, besides increased

of selectivity for CO₂ reduction was observed for Cobalt phthalocyanine with poly-4-vinyl pyridine polymers (CoPc – P₄VP) [25].

In this study, cellulose nanofibrils were functionalized with dicyanovinyl groups, from use ethoxymethylene-malononitrile (EMMN) as chemical modifier, for use in the electroreduction CO₂, whose excessive presence in the environment can cause serious problems, such as the greenhouse effect and, consequently, climate change [26, 27].

2. Method

2.1 Nanocellulose functionalization

In a flask, 0.5 g (3.1 mmol) by mass of an aqueous dispersion of 3% w/v CNFs (SuzanoPapel & Celulose) was placed under agitation. At that point, sodium hydroxide (NaOH) solution (0.1 M; Vetec; 97%) was added by means of a pipette (dropwise) until pH 10 was reached. The mixture was left under agitation for 30 minutes. Afterwards, EMMN (1.14 g; 9.3 mmol; Sigma Aldrich; 98%) was added to the mixture and left to react at room temperature (**Figure 2**), varying the reaction time and keeping the stoichiometry at 1:3 molar ratio (nanocellulose:malononitrile). The effect of stoichiometry and temperature on the reaction efficiency was evaluated for the best experimental condition.

After the programmed reaction time, the reaction medium was placed in a sintered glass funnel (no. 4) and rinsed with acetone (Vetec; 99.5%), ethanol (Vetec; 99.5%), methanol (Vetec; 99.8%), and distilled water until neutral pH was reached. The sample was then placed in an amber glass bottle and stored in a refrigerator.

2.2 Atomic force microscopy

AFM was conducted on a Dimension ICON microscope (Bruker). The sample was prepared by dripping 5 microliters of a solution containing the CNFs on a mica surface. The mica was cleaved twice right before applying the solution dropwise onto the surface and left to dry for 1 hour at room temperature. To prevent CNFs from dragging, intermittent contact mode with a rectangular silicon probe was used (cantilever spring constant = 40 N/m; oscillation frequency = 330 kHz).

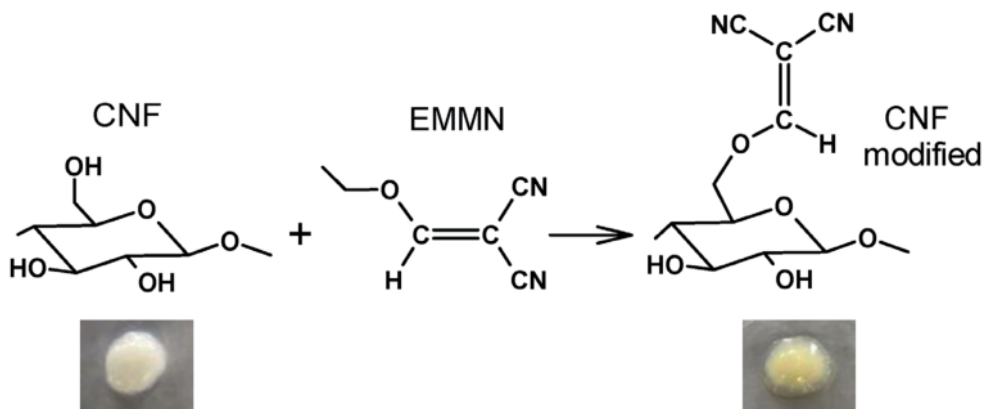


Figure 2.
CNF functionalization with EMMN.

2.3 Elementary analysis

The content of carbon (C), hydrogen (H), and nitrogen (N) in samples of pure and modified nanocellulose was determined by elementary analysis with a Perkin Elmer model 2400 instrument.

2.4 Thermal analysis

The thermogravimetric analysis (TG) of pure and modified nanocellulose was performed on a TG-DSC (Netzsch, model STA 409; PC – Luxx), with 50 mL min⁻¹ nitrogen flow, 25–720 °C analysis interval, and 10 °C min⁻¹ heating rate.

2.5 Electrochemical analysis

All electrochemical measurements were performed in a conventional three-electrode electrochemical cell. A platinum plate and Ag/AgCl were used as counter electrode and reference electrode, respectively. The working electrode comprised an ultrathin layer of catalyst (pure and modified nanocellulose) under the pyrolytic graphite layer (0.070 cm and 23.0 mm diameter) of a rotating disk electrode (RDE).

The 1% w/v aqueous suspension of pure and modified nanocellulose was prepared by ultrasonic dispersion in methanol. A 10 µL aliquot of this suspension was pipetted onto the surface of the pyrolytic graphite substrate. Then, the solvent was left to evaporate in a desiccator. Later, a 10 µL aliquot of Nafion® solution was pipetted onto the catalytic layer in order to attach the polymer layer to that of pyrolytic graphite.

The electrochemical behavior of pure and modified nanocellulose was monitored by means of cyclic voltammetry and polarization curves. The potentials applied to the electrodes during the assays were controlled by an Autolabpotentiostat/galvanostat. The electrolyte was saturated with pure argon (Ar) and CO₂ depending on the assay. Polarization curves were obtained using an RDE with potential ranging from –2.0 to 1.0 V vs. Ag/AgCl and a scanning rate of 5 mV s⁻¹.

3. Results and discussion

3.1 Atomic force microscopy

AFM images, **Figure 3**, reveal that the samples are organized as bundles of nanofibrils. In some places, individual nanofibrils can be found on the mica surface, which enabled measuring their diameter. **Figure 3a** and **c** show the relief images of the nanofibrils before and after chemical surface modification whereas **Figure 3b** and **d** show 3D AFM images. This analysis indicates that the average diameters of original nanofibrils and modified nanofibrils are 6.6 ± 1.6 nm and 5.6 ± 1.1 nm, respectively.

Overall, AFM results suggest that chemical modification has not changed the morphology of the nanofibrils, which exhibit diameters in the order of 6.0 nm.

3.2 Elementary analysis

Table 1 shows CHN results at several reaction times for the functionalization of CNFs with EMMN. This reaction occurs through nucleophilic vinylic substitution (SNV) of the ethoxy group with the malononitrile group in the polymer chain [28].

As shown in **Table 1**, the 8-hour reaction (Reaction 3) yielded the highest nitrogen content and is, therefore, the most effective in functionalizing and

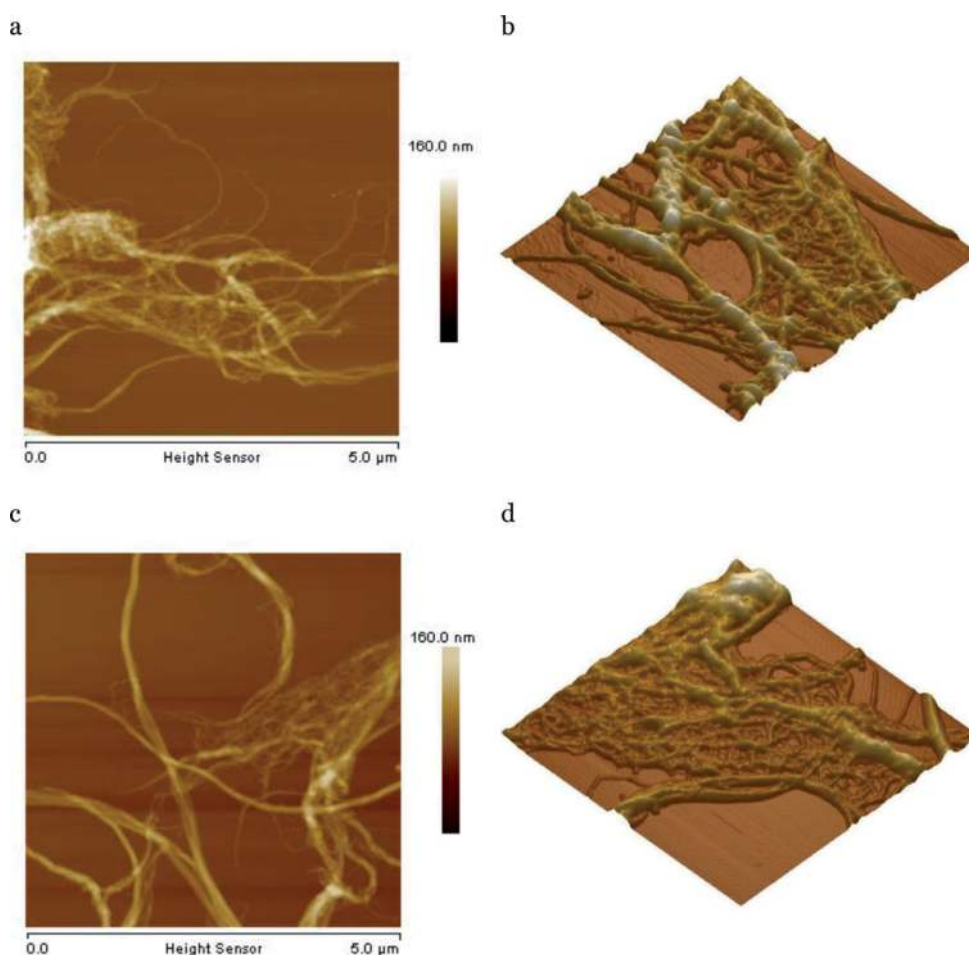


Figure 3. AFM for pure and modified CNFs in relief (a and c) and 3D (b and d - 2 microns × 2 microns × 15 nm), respectively.

Sample	Time (h)	C (%)	H (%)	N (%)
Pure nanocellulose	—	40.55	6.13	0.017
Reaction 1	2	40.66	5.69	0.280
Reaction 2	4	41.23	6.07	0.810
Reaction 3	8	38.86	5.50	0.920
Reaction 4	24	39.39	6.13	0.760

Table 1. Elementary analysis results for several times of reaction between CNFs and EMMN at 1:3 molar ratio and room temperature.

incorporating the malononitrile (dicyanovinyl) group into the nanocellulose chain. Increasing the reaction time to 24 h led to a decrease in nitrogen content, probably due to compound degradation.

For the best experimental condition (Reaction 3), the effect of stoichiometry and temperature on reaction yield was investigated. In this case, the same conditions used in Reaction 3 were used, with 1:2 stoichiometry at room temperature and, subsequently, 1:3 stoichiometry at 70 °C. Both assays exhibited a decrease in nitrogen content.

A more accurate way to measure reaction yield is by estimating the degree of substitution (DS), which can be obtained from Eq. (1):

$$DS = \frac{M_{glu} \cdot \%N}{100M_N - M_{mal} \cdot \%N} \quad (1)$$

Where DS is the degree of substitution, M_{glu} the molar mass of the glucose monomer (162 g/mol), M_N the molar mass of the nitrogen atom, M_{mal} the molar mass of the malononitrile group introduced into the cellulose (77 g), and %N the nitrogen content determined by elementary analysis.

By means of Eq. (1), Reaction 3 exhibits the highest DS value: 0.12. Despite not being very high, this value is close to those reported in the literature for reactions in which amino groups are introduced into the nanocellulose chain [29, 30]. For instance, the nitrogen content found in the functionalization reaction of cellulose nanocrystals with propargylamine was 0.79% [29]. Another study involving nanocellulose amination with 2-hydroxy-3-chloro-propylamine yielded a nitrogen content of 0.9% and a degree of substitution of 0.11 [30].

3.3 Thermal analysis

Figure 4 shows the thermogravimetric analysis for pure and modified CNFs as well as the derivatives of the thermogravimetric curves (dTG). The thermal behavior of both materials exhibits a single decomposition event between 305 °C and 390 °C, with pure CNFs exhibiting greater loss of mass at the end of the process (**Figure 4**). The peak corresponding to maximum mass loss for the functionalized CNFs occurs at a temperature approximately 20 °C lower ($T_{max} = 349.05$ °C) than that for pure CNFs ($T_{max} = 369.34$ °C), as shown in **Figure 3**. Similarly, the beginning of the decomposition process for the modified CNFs also occurs at a temperature approximately 20 °C lower ($T_{initial} = 306.21$ °C) than that for pure CNFs ($T_{initial} = 327.87$ °C).

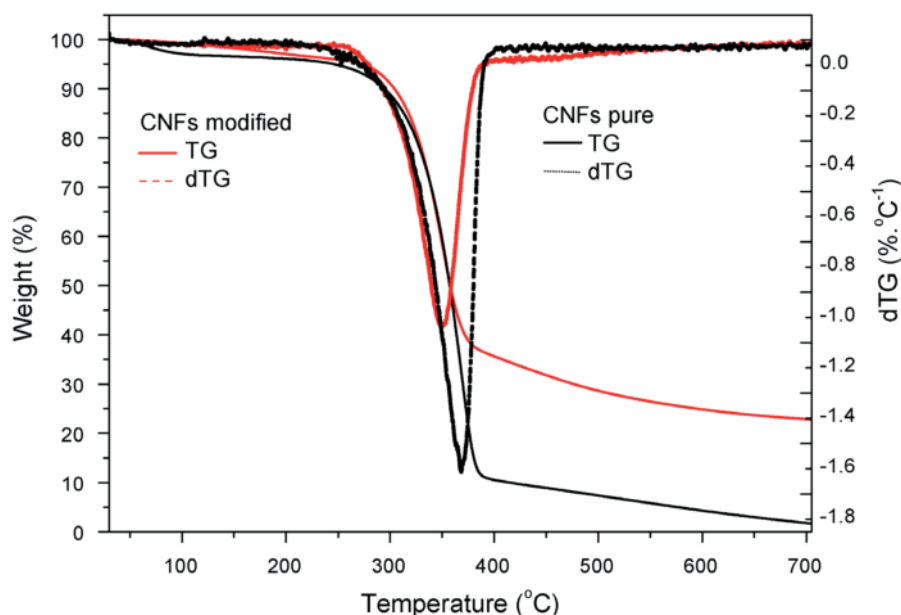


Figure 4.
TG and dTG curves for CNFs pure and modified.

The drop in the decomposition temperature of the modified CNFs may be due to a decrease in crystallinity when the dicyanovinyl group was introduced. There are reports in the literature of cellulose exhibiting lower thermal resistance when carbamate groups are introduced, which indicates a decrease in thermal stability of the functionalized cellulose as compared to that of pure cellulose [31].

3.4 Electrochemical analysis

Figure 5 shows cyclic voltammetry profiles for the CNFs electrocatalysts with and without modification at 5 mV/s scanning rate and applied potential ranging from -1.5 to 1.5 (vs Ag/AgCl). Conductivity of the electrocatalyst increases when cyan groups are introduced, as shown by the increase in area and current density.

This increase in conductivity has a positive effect concerning the use of the electrocatalyst as cathode in CO_2 reduction.

CO_2 conversion, whether thermal or electrochemical, is associated with high energy consumption due to CO_2 being a very stable molecule. In the case of electrochemical reduction of CO_2 , the source of energy is electricity. It is possible to reduce CO_2 completely by applying a higher potential. However, an appropriate catalyst can significantly reduce energy consumption and increase end-product selectivity.

Figure 6 shows the polarization curves for pure and modified CNFs in an atmosphere of Ar and CO_2 . It is possible to observe that CNFs modification with cyan groups increases current density of the CO_2 reduction reaction, which implies a higher CO_2 conversion rate in the products. It also points to the onset potential for CO_2 reduction shifting to more positive values as compared to those observed for pure CNFs. This may be attributed to adsorption/desorption of reaction intermediates in the polymer interface due to the presence of the cyan group.

The use of CNFs modified by the dicyan group has improved the catalytic efficiency of the electrocatalyst, thereby promoting CO_2 reduction, probably due to higher availability of active sites in its fibrillar structure, especially cyan groups on the surface.

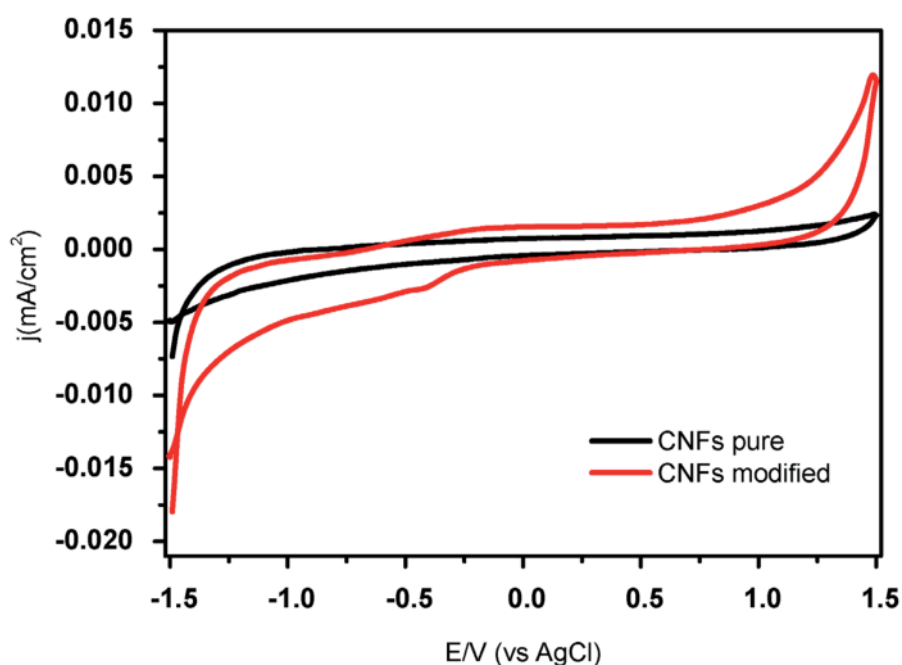


Figure 5. Cyclic voltammetry for CNFs pure and modified at a scanning rate of 5 mV s^{-1} ; electrolyte: K_2SO_4 0.5 Mol/L saturated with Ar at 25°C . currents normalized by the geometric area of the electrode.

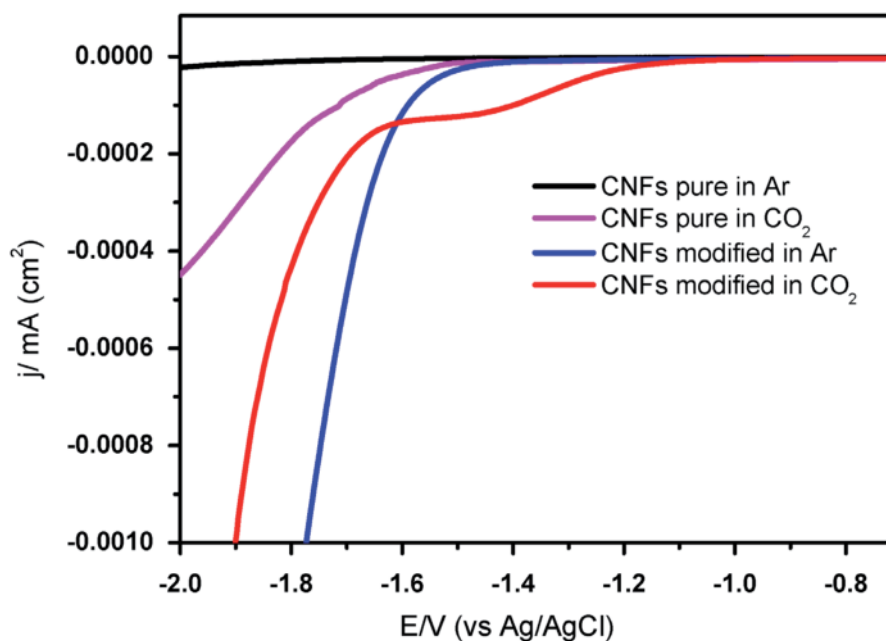


Figure 6. Steady-state polarization curves for electrodes containing CNFs pure and modified at a scanning rate of 5 mV s^{-1} , K_2SO_4 0.5 Mol/L saturated with Ar and CO_2 at 25°C . currents normalized by the geometric area of the electrode.

4. Conclusion

AFM results indicate no significant changes in the morphology of modified cellulose nanofibrils. The best experimental conditions for chemical functionalization is 1:3 molar ratio at room temperature. As reported in other studies on chemically modified cellulose, the degradation temperature for modified cellulose nanofibrils is lower than that for pure cellulose.

From the electrochemical perspective, introducing dicyanovinyl groups into the polymeric chain of cellulose nanofibrils has led to significantly higher electrocatalytic activity in CO_2 reduction as compared to that for pure cellulose nanofibrils, shifting the onset potential to more positive values as compared to that observed for the reaction with Ar. Moreover, the CO_2 molecule exhibits affinity for the cellulose polymer and the polymeric layer may play an inhibitory role in water reduction.

Acknowledgements

The authors thanks the Program of Post Graduation in Science of Materials - PPGCM of the Universidade Federal de São Carlos - UFSCar, campus Sorocaba for financial support.

Conflict of interest

The authors declare no conflict of interest.

Author details

Robson V. Pereira¹, Thais E. Gallina¹, Marcelo A. Pereira-da-Silva², Kênia S. Freitas¹ and Aparecido J. de Menezes^{3*}


1 Grupo de Eletroquímica e Polímeros Naturais (GEPN), Universidade Federal do Rio de Janeiro - UFRJ, Campus Macaé, Macaé - Rio de Janeiro, Brasil

2 Instituto de Física de São Carlos, IFSC, Universidade de São Paulo - USP, São Carlos, São Paulo, Brasil

3 Grupo de Polímeros de Fontes Renováveis - GPFR, Universidade Federal de São Carlos - UFSCar, Campus Sorocaba, Sorocaba, São Paulo, Brasil

*Address all correspondence to: jrmenezes@ufscar.br

IntechOpen

© 2021 The Author(s). Licensee IntechOpen. This chapter is distributed under the terms of the Creative Commons Attribution License (<http://creativecommons.org/licenses/by/3.0>), which permits unrestricted use, distribution, and reproduction in any medium, provided the original work is properly cited. 

References

- [1] Habibi Y. Lucia L. A. Rojas O. J. Cellulose Nanocrystals: Chemistry, Self-Assembly, and Applications. *Chem. Rev.* 2010;110:3479-3500. DOI: 10.1021/cr900339w
- [2] Alavi M. Modifications of microcrystalline cellulose (MCC), nanofibrillated cellulose (NFC), and nanocrystalline cellulose (NCC) for antimicrobial and wound healing applications. *e-Polymers.* 2019;19:103-119. DOI: 10.1515/epoly-2019-0013
- [3] Fengel D. Wegener G. *Wood: chemistry, ultrastructure and reactions.* Berlin: Walter de Gruyter; 1984. 613 p.
- [4] Blanco A. et al. Nanocellulose for Industrial Use: Cellulose Nanofibers (CNF), Cellulose Nanocrystals (CNC), and Bacterial Cellulose (BC). In: Hussain C. M. *Handbook of Nanomaterials for Industrial Applications.* 2018. p. 74-126. DOI: 10.1016/b978-0-12-813351-4.00005-5
- [5] Abitbol T. et al. Nanocelulose, a tiny fiber with huge applications, *Curr. Opin. In Biotech.* 2016;39:76-78. DOI: 10.1016/j.copbio.2016.01.002
- [6] Thompson L. et al. Cellulose nanocrystals: Production, functionalization and advanced applications. *Rev. Adv. Mater. Sci.* 2019;58: 1-16. DOI: 10.1515/rams-2019-0001
- [7] Dufresne A. Cellulose nanomaterial reinforced polymer nanocomposites. *Current Opinion in Colloid & Interface Science,* 2017;29:1-8. DOI: 10.1016/j.cocis.2017.01.004
- [8] Gan P. G. et al. Thermal properties of nanocellulose-reinforced composites: A review, *J. Appl. Polym. Sci.* 2020;137:48544-48558. DOI: 10.1002/app.48544
- [9] Mondal S. Review on Nanocellulose Polymer Nanocomposites. *Polymer-Plastics Techn. and Eng.* 2018;57:1377-1391. DOI: 10.1080/03602559.2017.1381253
- [10] France K. J. Hoare T. Cranston, E. D., Review of hydrogels and aerogels containing nanocellulose, *Chem. Mater.* 2017;29:4609-4631. DOI: 10.1021/acs.chemmater.7b00531
- [11] Long L. Y. Weng Y. X. Wang Y.Z. Cellulose aerogels: Synthesis, applications and prospects. *Polymers.* 2018;10:1-28. DOI: 10.3390/polym10060623
- [12] Patel D.K. Duttav S. D. Lim K. T. Nanocellulose-based polymer hybrids and their emerging applications in biomedical engineering and water purification. *RSC. Adv.* 2019;9:19143-19162. DOI: 10.1039/C9RA03261D
- [13] Ngwabebhoh F. A. Yildiz U. Nature-derived fibrous nanomaterial toward biomedicine and environmental remediation: Today's state and future prospects. *J. Appl. Polym. Sci.* 2019;136:47878. DOI: 10.1002/app.47878
- [14] Akhlaghi S. P. Berry R. C. Tam K. C., Surface modification of cellulose nanocrystal with chitosan oligosaccharide for drug delivery applications, *Cellulose.* 2013;20:1747-1764. DOI: 10.1007/s10570-013-9954-y
- [15] Liu L. et al. Adsorption removal of dyes from single and binary solutions using a cellulose-based bioadsorbent. *ACS Sustainable Chem. Eng.* 2015;3:432-442. DOI: 10.1021/sc500848m
- [16] Zhang Y. et al. Electrochemical chiral sensor based on cellulose nanocrystals and multiwall carbon nanotubes for discrimination of tryptophan enantiomers. *Cellulose.* 2018;25:3861-3871. DOI: 10.1007/s10570-018-1816-1

- [17] Cheng Q. et al. Construction of transparent cellulose-based nanocomposite papers and potential application in flexible solar cells, *ACS Sustainable Chem. Eng.* 2018;6:8040-8047. DOI: 10.1021/acssuschemeng.8b01599
- [18] Hsu H. H. Zhong W. Membranes for Free-Standing Supercapacitors Nanocellulose-Based Conductive: A Review. *Membranes.* 2019;9:1-21. DOI: 10.3390/membranes9060074
- [19] Pereira R. V. Ferreira A. P. G. Gehlen M. H. Fluorescent probes with malononitrile side group in methyl methacrylate copolymers. *J. of Photochem. and Photobiol. A, Chem.* 2008,198:69-74. DOI: 10.1016/j.jphotochem.2008.02.017
- [20] Pereira R. V. Gehlen M. H. Polymerization and Conformational Transition of Poly(methacrylic Acid) Probed by Electronic Spectroscopy of Aminoacridines. *Macromolecules* 2007,40:2219-2223. DOI: 10.1021/ma062020c
- [21] Karamad M. et al. Mechanistic Pathway in the Electrochemical Reduction of CO₂ on RuO₂. *ACS Catalysis.* 2015;5:4075-4081. DOI: 10.1021/cs501542n
- [22] Jhong H. M. Ma S. Kenis P. Electrochemical conversion of CO₂ to useful chemicals: current status, remaining challenges, and future opportunities. *Curr. Op. in Chem. Eng.* 2013;2:191-199. DOI: 10.1016/j.coche.2013.03.005
- [23] Zhang S. et al. Polyethylenimine-Enhanced Electrocatalytic Reduction of CO₂ to Formate at Nitrogen-Doped Carbon Nanomaterials. *J. Am. Chem. Soc.* 2014;136:7845-7848. DOI: 10.1021/ja5031529
- [24] Aydin R. Köleli F. Electrochemical reduction of CO₂ on a polyaniline electrode under ambient conditions and at high pressure in methanol. *J. Electroanal. Chem.* 2002;535:107-112. DOI: 10.1016/S0022-0728(02)01151-8
- [25] Liu Y. McCrory C.C.L. Modulating the mechanism of electrocatalytic CO₂ reduction by cobalt phthalocyanine through polymer coordination and encapsulation. *Nat. Commun.* 2019;10:1683 DOI: 10.1038/s41467-019-09626-8
- [26] Hu J. P. et al. Sensitivity analysis of greenhouse effect with the concentration changes of greenhouse gases. *J. of Eng. Thermophysics.* 2012;33:1380-1382.
- [27] Goldemberg J. *Energia e Desenvolvimento Sustentável.* São Paulo: Blucher, 2010; 4: 124-126.
- [28] Salon J. et al. Nucleophilic vinylic substitution (SNV) of activated alkoxyethylene derivatives with 6-aminoquinoxaline. *Eur. J. Org. Chem.* 2005; 4870-4878. DOI: 10.1002/ejoc.200500298
- [29] Filpponen I., Sadeghifar H., Argyropoulos, D. S. Photoresponsive cellulose nanocrystals, *Nanomater. Nanotechnol.* 2011;1:34-43. DOI: 10.5772/50949
- [30] Akhlaghi S P. et al. Synthesis of amine functionalized cellulose nanocrystals: optimization and characterization, *Carbohydr. Res.* 2015;409: 48-55. DOI: 10.1016/j.carres.2015.03.009
- [31] Vo L.T. et al. Functionalisation of cellulosic substrates by a facile solventless method of introducing carbamate groups. *Carbohydr. Polym.* 2010;82:1191-1197. DOI: 10.1016/j.carbpol.2010.06.052